Molecular Modeling of Saccharides, 6[1]

Small-Ring Cyclodextrins: Their Geometries and Hydrophobic Topographies☆

Stefan Immel[a], Jürgen Brickmann[b], and Frieder W. Lichtenthaler*[a]

Institut für Organische Chemie der Technischen Hochschule Darmstadt[a], Petersenstraße 22, D-64287 Darmstadt

Institut für Physikalische Chemie der Technischen Hochschule Darmstadt[b], Petersenstraße 20, D-64287 Darmstadt

Received December 27, 1994

Key Words: Cyclodextrins, small-ring / Molecular geometries / Molecular lipophilicity patterns / Inclusion complexes

A detailed force-field-based evaluation of the molecular geometries of small-ring cyclodextrins **1**–**3** with three, four, and five α(1→4)-linked glucose residues and the starch-derived α-cyclodextrin (**4**) was performed by using molecular mechanics and high-temperature annealing. The resulting minimum-energy structures reveal that the progressive strain imposed by diminution of the cyclodextrin macrocycle from six glucose units (α-CD, **4**) to five (cycloglucopentaoside **3**), four (tetraoside **2**), and three (cyclotrioside **1**) is reflected in a widening of the intersaccharidic bond angle, in a complex balance of the interrelated glucose tilt angles τ and the glycosidic torsions Φ and Ψ against each other, and most strikingly, in a specific unilateral distortion of the pyranoid rings, i.e. flattening at C-4 towards the E_1 envelope conformation. This successive levelling at C-4, induced by a decrease of the two related ring torsion angles, is small in the pentamer **3**, pronounced in **2**, and fully realized in the cyclotrioside **1**. – The respective contact surfaces of the minimum-energy conformers and their molecular lipophilicity patterns (MLP), in color-coded form, were also generated, allowing an assessment of their capabilities to form inclusion complexes. Accordingly, only the cyclopentaoside **3** exhibits a hydrophobic central cavity similar to that of α-CD (**4**), the smaller cyclodextrins **2** and **1** are closed, yet contain a hydrophobic indentation for potential binding.

The native cyclodextrins **4**–**7** obtained from the action of *Bacillus macerans* amylase on starch, are cyclic oligosaccharides composed of six, seven, eight or nine α(1→4)-linked D-glucopyranose units[2]. All of these are characterized by their X-ray structures[3,4], and a large body of information has accumulated on their ability to incorporate a variety of organic compounds into their cavity, both in the solid-state and in solution[2].

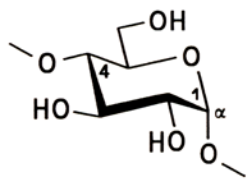

Small-ring cyclodextrins:

1 *cyclo*[D-Glc*p* α(1→4)]$_3$
2 *cyclo*[D-Glc*p* α(1→4)]$_4$
3 *cyclo*[D-Glc*p* α(1→4)]$_5$

Starch derived cyclodextrins:

α-CD **4** *cyclo*[D-Glc*p* α(1→4)]$_6$
β-CD **5** *cyclo*[D-Glc*p* α(1→4)]$_7$
γ-CD **6** *cyclo*[D-Glc*p* α(1→4)]$_8$
δ-CD **7** *cyclo*[D-Glc*p* α(1→4)]$_9$

Although the cyclodextrin series may extend on the high-molecular weight side beyond the δ-cyclodextrin **7**[5,6], no evidence has been brought forth that a cyclodextrin with fewer than six glucose units – as, e.g. the cycloglucopentaoside **3** – is present in the amylose digestions of starch[5]. This abrupt termination of the series on the low-molecular weight side has, over the years, been commented in various ways. French, in 1957, remarked that the smallest cyclodextrin ring which can be constructed with space-filling models on the basis of $^4C_1$ conformations of the glucose units is the α-cyclodextrin (**4**); however, when allowing boat or twist conformations for the pyranoid rings, "it is possible to construct essentially strainless cycloamylose rings having any number of D-glucose units from three to infinity"[5]. In 1970, on the basis of potential energy calculations it was inferred, that "there is a drastic increase in energy when the number of D-glucose residues is fewer than six"[7], which was attributed to the fact that the diameter of a cyclodextrin with five or less sugar units cannot accommodate the 6-CH_2OH groups, which point approximately to the interior[7]. As recent as 1992, the non-existence of a cyclodextrin with less than six glucose units was rationalized to be due to "the high internal tensions which could then appear at the level of the ring"[8].

Whilst the glycosyltransferase from *Bacillus macerans* is obviously unable to generate cyclodextrins with fewer than six glucose units from starch, chemical synthesis is not, as convicingly evidenced by the recent straightforward preparation of the pentametric α(1→4)-linked cyclodextrin **3** via cyclization of a linear glucopentaose derivative[9]. In a simi-

  0947–3440/95/0606–0929 $ 10.00+.25/0

lar fashion, the respective cyclomannin pentamer, i.e. the α(1→4)-linked all-*manno* analog of **3**, has been synthesized[10,11].

Accordingly, the early considerations of small-ring cyclodextrins[5–8] were obviously premature in their general as well as specific implications. This prompted us to subject the cyclodextrins **1**–**3** composed of three, four, and five glucose units, respectively, to a detailed molecular modeling study, knowledge of their geometries and molecular lipophilicity patterns (MLP) conceivably allowing an assessment of their host-guest complexation capabilities.

Nomenclature: Recently, a uniform nomenclature consistent with the present naming of oligosaccharides has been proposed[12], which entails considerable simplifications in the exasperating task of naming these compounds, and accordingly has already received authoritative recognition[13].

The new nomenclature retains the term cyclodextrin – dextrose was an early synonym for glucose – for all cyclooligosaccharides composed of glucose units, irrespective of their intersaccharidic linkages. As a logical extension, cyclic oligosaccharides consisting of mannose, galactose, or fructose are correspondingly named cyclomannins, cyclogalactins, and cyclofructins.

The traditional names for the starch-derived cyclodextrins use Greek letters for their differentiation, i.e. α-CD through δ-CD (**4**–**7**) for those containing 6–9 glucose units. Whilst this is standard usage, and hence to be maintained, it appears unreasonable to adhere to the Greek alphabet with other cyclooligosaccharides, not only because this does not reveal ring size or the number of sugar units in a direct way, but it runs into basic difficulties in naming cyclodextrins or analogs smaller than α, as for example, **1**, **2**, and **3**. Furthermore, chemical names such as cyclomaltohexaose for the α-cyclodextrin (**4**) induce confusion as to the number of maltose units in the ring (six?), and the ending -ose (instead of -oside for cyclic oligoglucoside) which signifies a free anomeric center.

To establish consistency, the new terminology[12] entails for all cyclodextrins the term cycloglucooligosaccharide with the number of glucose units and the type of intersaccharidic linkage inserted as the specific designation. This leads in a straightforward manner to the simple nomenclature outlined in Table 1, in which – except for **1**, **2**, and the cyclogalactin – all compounds are known[2,4,9,11,15–19].

Most notably, the small-ring cyclodextrins **1**–**3**, subject of this account, smoothly emerge therefrom as cycloglucotrioside, tetraoside, and pentaoside.

Conformational Features of the Cyclodextrins 1–4

The global conformation and the total molecular energy of the cyclodextrins depend on all the intersaccharidic torsion angles Φ and Ψ as well as on the tilt angles τ of the individual glucose units[20] that denote their inclination in relation to the macrocycle (cf. Figure 1), while the pyranoses itself are comparatively rigid; all those molecular parameters are interrelated in a complex manner. For symmetrical structures, the internal degrees of freedom which have to be taken into consideration are considerably reduced, since then Φ and Ψ become an explicit function of τ. The torsion angles ω (Figure 1) describe the orientation of the 6-OH groups with respect to the pyranoid ring, and thus are related to local conformational aspects.

Geometry analysis of the small-ring cyclodextrins **1**–**3** was performed by molecular mechanics by using the PIMM91 force-field program[21] (cf. Experimental); thereby the native α-cyclodextrin (**4**) – despite the availability of crystal structural data for different forms of its hydrate[22], and several molecular mechanics[23] and dynamics studies[24] – was included to unequivocally draw parallels to its small-ring isomers independent of the mode of previous analyses. Of the various relevant variables that may be subjected to systematic permutation, we selected the tilt angle τ, denoting the inclination of the pyranoid rings towards the mean plane of the cyclodextrin macrocycle (Figure 1), and the torsion angle ω describing the conformation of the primary 6-OH in relation to the pyranoid ring (Figure 1); after each step, the molecular geometries were fully energy-optimized.

Table 1. Simplified designation of cyclooligosaccharides based on the IUPAC/IUB-approved abbreviations[14] of linear oligosaccharides

Generic name	Specific name		Abbreviation	Ref.
cyclodextrin	cyclo-α(1→4)-glucotrioside	(**1**)	*cyclo*[Glc*p*α(1→4)]$_3$	–
cyclodextrin	cyclo-α(1→4)-glucotetraoside	(**2**)	*cyclo*[Glc*p*α(1→4)]$_4$	–
cyclodextrin	cyclo-α(1→4)-glucopentaoside	(**3**)	*cyclo*[Glc*p*α(1→4)]$_5$	[9]
α-cyclodextrin	cyclo-α(1→4)-glucohexaoside	(**4**)	*cyclo*[Glc*p*α(1→4)]$_6$	[2]
δ-cyclodextrin	cyclo-α(1→4)-gluconononaoside	(**7**)	*cyclo*[Glc*p*α(1→4)]$_9$	[4]
cyclodextrin	cyclo-α(1→6)-glucotrioside		*cyclo*[Glc*p*α(1→6)]$_3$	[15]
cyclodextrin	cyclo-α(1→6)-glucohexaoside		*cyclo*[Glc*p*α(1→6)]$_6$	[15]
cyclodextrin	cyclo-β(1→3)-glucohexaoside		*cyclo*[Glc*p*β(1→3)]$_6$	[16]
α-cyclomannin	cyclo-α(1→4)-mannohexaoside		*cyclo*[Man*p*α(1→4)]$_6$	[17]
β-cycloaltrin	cyclo-α(1→4)-altroheptaoside		*cyclo*[Alt*p*α(1→4)]$_7$	[18]
α-cyclogalactin	cyclo-β(1→4)-galactohexaoside		*cyclo*[Gal*p*β(1→4)]$_6$	–
cyclolactin	cyclo-α(1→4')-lactotrioside		*cyclo*[Gal*p*β(1'→4) Glc*p*α(1→4')]$_3$	[11]
α-cyclofructin	cyclo-β(1→2)-fructohexaoside		*cyclo*[Fru*f*β(1→2)]$_6$	[19]

Figure 1. Cyclodextrin geometry descriptors: the intersaccharidic bond angle φ is defined by the atoms $C_1-O_1-C_{4'}$, the torsion angles which describe the conformations about the glycosidic linkages are denoted as Φ ($O_5-C_1-O_1-C_{4'}$) and Ψ ($C_1-O_1-C_{4'}-C_{3'}$). The endocyclic ring torsions around C-4 are designated as Θ_1 ($C_2-C_3-C_4-C_5$) and Θ_2 ($C_3-C_4-C_5-O_5$), the exocyclic torsion angle ω ($O_5-C_5-C_6-O_6$) describes the orientation of the primary 6-OH relative to the pyranoid ring, whereby the three staggered conformations are referred to as *gauche-gauche* (*gg*, ω ≈ −60°), *gauche-trans* (*gt*, ω ≈ +60°), and *trans-gauche* (*tg*, ω ≈ ±180°). The tilt angle τ denotes the inclination of the pyranose rings toward the macrocyclic ring perimeter, i.e. the angle between the cyclodextrin mean plane of all intersaccharidic (i.e. anomeric) oxygen atoms versus the least-squares best-fit mean plane through the six pyranoid ring atoms ($C_1-C_2-C_3-C_4-C_5-O_5$, bottom plot; hydrogen atoms are omitted for clarity); the normal vector *g* of the latter plane always points to the outside of the macrocycle[20]. Absolute values of $|\tau| > 90°$ indicate the 6-CH_2OH side to be turned towards the central cavity; a positive sign of τ indicates the upper face (clockwise view on C_1-C_5 and O_5) of the sugar moieties pointing towards the outside of the macrocyclic ring

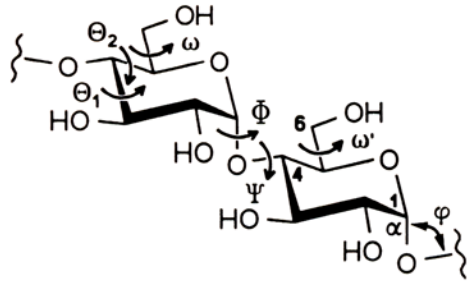

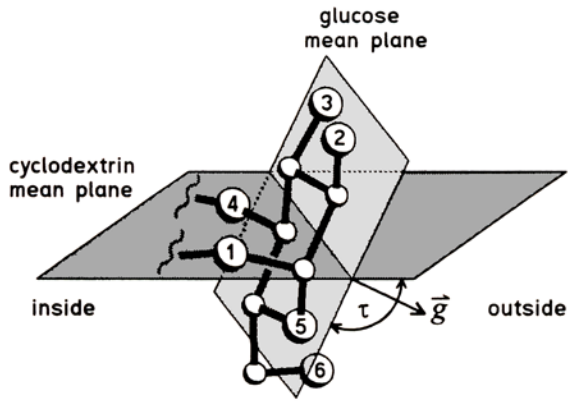

The molecular parameters obtained in this way for the minimum-energy conformations of **1**−**4** are listed in Table 2, the resulting overall geometries are depicted in Figure 2, onto which, in addition, the MOLCAD program[25] generated contact surfaces[26] were superimposed. As a consequence of the structure generation procedure, the PIMM91 minimum-energy geometries exhibit symmetrical, almost perfectly planar *n*-polygons of the O-1 atoms (root-mean-square displacements from planarity <0.002 Å), and hence can be regarded as the respective time-averaged "molecular images" of solution conformations.

In the case of α-cyclodextrin (**4**), the ball-and-stick model representation, and in more detail, the calculated data in Table 2, reveal an essentially unstrained, torus-shaped macrocycle, with the primary 6-OH groups located on one side of the molecule, whilst the opposite aperture is made up by the secondary 2-OH and 3-OH groups. The intersaccharidic bond angle φ ($C_1-O_1-C_{4'}$) as well as the glycosidic torsion angles Φ and Ψ are within normal ranges. Good agreement is also observed for the alternate torsions Φ′ ($H_1-C_1-O_1-C_{4'}$) and Ψ′ ($C_1-O_1-C_{4'}-H_{4'}$) based on the ^{13}C-/^1H-NMR coupling constants in $CDCl_3$ solution of the peracetate of **4**[27]; in particular, both the experimental and theoretical methodology estimate Ψ to be approximately 20−30° larger than Φ (Φ ≈ Φ′ + 120° and Ψ ≈ Ψ′ + 120°). The same holds for the tilt angle τ, its mean value of 109° clearly indicating the pyranoid rings to be inclined such that their 6-CH_2OH portions re turned towards the center cavity, forming the smaller opening, whilst the 2-OH/3-OH section points away from the molecular axis, moulding the wider torus rim.

The pyranoid rings in α-cyclodextrin (**4**) adopt a standard $^4C_1$ conformation as evidenced by the Cremer-Pople (CP) puckering parameters[28−30] and the torsion angles within the pyranose rings − only two, namely Θ_1 and Θ_2, describing the conformational relationships around C-4, are listed in Table 2 − that exhibit usual values ($\Theta_1 \approx +47°$ and $\Theta_2 \approx -47°$). These calculated results are well corroborated by the data obtained from statistical analysis of altogether 46 different solid-state structures of α-cyclodextrin and its inclusion complexes as retrieved from the Cambridge Crystallographic Data File[31,32] (cf. Table 2).

On proceeding from α-cyclodextrin (**4**) to the smaller cyclodextrins **1**−**3** by successive excision of one glucose unit from the macrocycle, the variables that are balanced against each other are the intersaccharidic bond angle φ, the glycosidic torsion angles Φ and Ψ, the tilt angle of the pyranoid rings (τ), and the puckering of the glucose rings. The extent to which each of these parameters is affected in the calculatory energy-minimum structures is revealed by the data in Table 2. The $C_1-O_1-C_4$ bond angle φ is successively widened with minor effects in the cycloglucopentaoside (**3**) and the tetramer (**2**, Δφ ≈ +2°), versus a sizeable 6° strain [from φ ≈ 117.3° in α-CD (**4**) to 123.5°] in the cycloglucotrioside **1**. Similar small reverberations are observed for the inclination of the pyranoid rings towards the center cavity, i.e. the tendency of the hydroxymethyl groups to be canted towards the center axis is uniformly maintained throughout the entire series. The tilt angles τ show only minor variations when proceeding from **4** → **1**, whilst the glycosidic torsion angles show opposite trends, Φ decreasing (≈100° → ≈80°) with increasing Ψ (≈135° → ≈155°); thus, the geometrical constraints introduced into the macrocycle by reducing the glucose units from six to five, four, and three express themselves in a balancing of the three variables τ, Φ, and Ψ against each other. The values enforced in the cycloglucotrioside **1** are such, however, that an immense strain is to be surmised in the macrocycle, conceivably so high that the chances for this molecule to be synthesized are rather dim.

Another major effect in compensating the geometrical constraints imposed on the cyclooligoglucosides when proceeding from six to three glucose units are the changes in pyranose conformations. The essentially normal $^4C_1$ chair in the glucose portions of α-cyclodextrin (**4**) is only slightly

Table 2. Mean molecular geometry parameters of calculated cyclodextrin structures with three (**1**), four (**2**), five (**3**), and six (**4**, α-CD) glucose units in α(1→4)-linkages (root-mean-square deviations in parentheses). For α-cyclodextrin (**4**), the experimental data obtained from statistical analysis of crystal structures were included for comparison

Cyclodextrin	Intersaccharidic torsion angles[a]		bond angle[b]	Tilt angle[c]	Atomic distances [Å]		
	$<\Phi>$	$<\Psi>$	$<\varphi>$	$<\tau>$	$<O_1\text{-}O_{1''}>$[d]	$<O_2\text{-}O_{3'}>$	$<C_6\text{-}C_{6'}>$
Solid-state structural data[e]:							
4 (α-CD)	107.4(6.6)	130.7(8.5)	118.2(2.0)	102.1(7.1)	8.51(0.23)	3.06(0.55)	4.45(0.21)
PIMM91 analysis[f]:							
4 (α-CD)	95.4(0.3)	138.7(1.1)	117.3(0.2)	109.0(0.2)	8.74(0.03)	3.30(0.04)	4.19(0.01)
3	102.4(0.7)	133.2(1.1)	117.8(0.2)	101.7(0.6)	6.53(0.02)	3.21(0.06)	4.51(0.01)
2	92.4(1.0)	141.0(0.7)	119.2(0.2)	104.6(0.7)	5.30(0.02)	3.75(0.07)	4.49(0.01)
1	81.7(0.1)	156.5(0.1)	123.5(0.1)	105.3(0.1)	3.32(0.01)	4.62(0.01)	4.74(0.01)
CHARMM HTA study[g]:							
4 (α-CD)	131. (11.)	111. (11.)	113.1(0.2)	85.7(10.)	8.21(0.08)	2.64(0.03)	5.23(0.35)
3	128. (10.)	113. (11.)	114.0(0.3)	88.7(8.6)	6.31(0.15)	2.73(0.35)	5.22(0.34)

Cyclodextrin	Pyranoid ring torsion angles[a]		Pyranose Cremer-Pople parameters[28-30]			Glucose conformation
	$<\Theta_1>$	$<\Theta_2>$	$<Q>$	$<\theta>$	$<\phi>$	
Solid-state structural data[e]:						
4 (α-CD)	52.3(5.1)	-53.0(6.2)	0.577(0.036)	5.7(4.8)	–[h]	$^4C_1$
PIMM91 analysis[f]:						
4 (α-CD)	46.9(0.7)	-47.0(0.2)	0.550(0.002)	9.0(0.3)	74.3(6.1)	$^4C_1$
3	39.4(0.9)	-39.6(0.1)	0.544(0.004)	18.0(0.2)	67.1(4.8)	$^4C_1$ (→ E_1)
2	30.5(0.3)	-28.6(0.4)	0.546(0.004)	28.9(0.3)	69.3(1.6)	E_1 (→ $^4C_1$)
1	11.8(0.1)	-6.1(0.1)	0.585(0.001)	48.8(0.1)	70.8(0.1)	E_1
CHARMM HTA study[g]:						
4 (α-CD)	45.5(1.7)	-49.9(1.4)	0.620(0.007)	14.8(1.4)	39.1(6.9)	$^4C_1$
3	39.0(2.3)	-43.5(2.6)	0.614(0.005)	20.9(2.1)	44.1(5.0)	$^4C_1$ (→ E_1)

[a] Φ: $O_5-C_1-O_1-C_{4'}$, Ψ: $C_1-O_1-C_{4'}-C_{3'}$, Θ_1: $C_2-C_3-C_4-C_5$, Θ_2: $C_3-C_4-C_5-O_5$. – [b] φ: $C_1-O_1-C_{4'}$. – [c] Angle between best-fit mean plane of the macroring (defined by all O_1'' atoms) and each glucose-mean plane (atoms C_1 to C_5 and O_5). – [d] O_1-O_1'' distances (in Å) diagonal across the cyclodextrin ring. – [e] Experimental values from 46 different solid-state structures of α-cyclodextrin and its inclusion complexes, including 54 crystallographically independent molecules. – [f] Calcd. (PIMM91) for almost symmetrical, global minimum-energy structures found. – [g] Calcd. (CHARMM, High-Temperature Annealing), Boltzmann weighting of all HTA structures. – [h] For $\theta \rightarrow 0°$, the puckering angle ϕ becomes meaningless, since $^4C_1$ conformations are identical to $^2C_5$ and $^0C_3$.

distorted in the pentameric **3**: a slender flattening at C-4 towards the E_1 envelope, as indicated by the diminution of the two ring torsion angles (absolute values decrease by ca. 7° each for Θ_1 and Θ_2), and the pyranose puckering parameters[33]. This trend continues more pronouncedly in the tetraoside **2** and reaches an essentially full E_1 envelope in the trioside **1** with Θ values of +12° and −6° only, and is also manifested in the Cremer-Pople parameters[28,29]: the puckering amplitude Q, i.e. the atomic mean-square deviation form planarity, is slightly higher in **1** (≈0.59 Å) than in **2**–**4** (≈0.55 Å). Most notably, the parameter θ representing the latitude deviation of the spherical polar coordinate set [Q, θ, ϕ] changes from ca. 5–10° in the case of α-cyclodextrin (**4**) to ca. 49° in the cycloglucotrioside **1**, while the nearly constant longitude of $\phi \approx 65-75°$ indicates bending to occur particularly at C-4[30].

In a more transparent illustration, this trend from $^4C_1 \rightarrow E_1$ conformations may be described by the "overall kink angle" ε, defined as the angle between the C_1-O_1 and C_4-O_4 bond vectors of the respective glucose residues (cf. Table 3). The contraction of the macrocycle forces ε to become successively smaller, from 65° in α-cyclodextrin (**4**) to 50° in the pentamer **3**, and to 37 and 19° in the cycloglucotetraoside **2** and trioside **1**, respectively.

In this context, it is to be noted that the increasing steric strain when going from the hexamer to the trimer expresses itself in flattening at C-4 via decrease of the two related ring torsion angles Θ_1 and Θ_2, and not – at least not appreci-

Figure 2. Ball-and-stick model representations of the minimum-energy structures (PIMM91) and dotted contact surfaces of the cyclodextrins **1**–**4** containing three, four, five, and six α(1→4)-linked glucose units, respectively. Structures are shown perpendicular to the mean ring plane of the macrocycles and are viewed through the large opening of the conically shaped molecules, i.e. the 2-OH/3-OH side of the pyranoid rings points towards the viewer, and the primary 6-CH_2OH groups away from him, towards the back; oxygen atoms are shaded

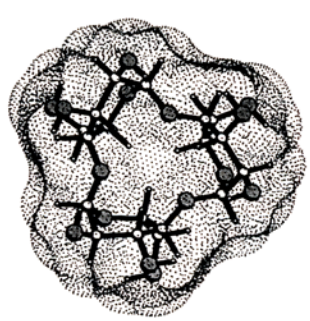

cyclo[D-Glc*p* α(1→4)]$_3$
1

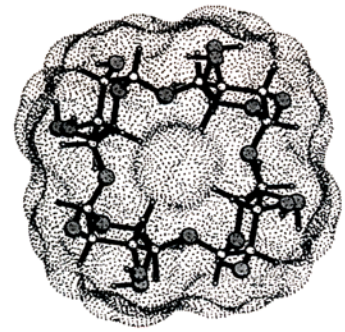

cyclo[D-Glc*p* α(1→4)]$_4$
2

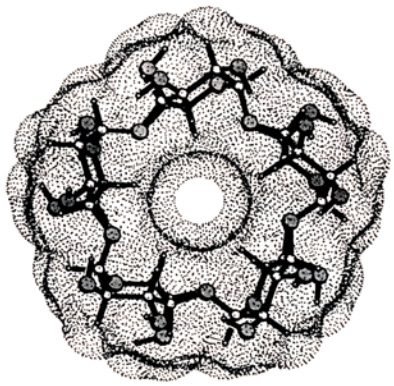

cyclo[D-Glc*p* α(1→4)]$_5$
3

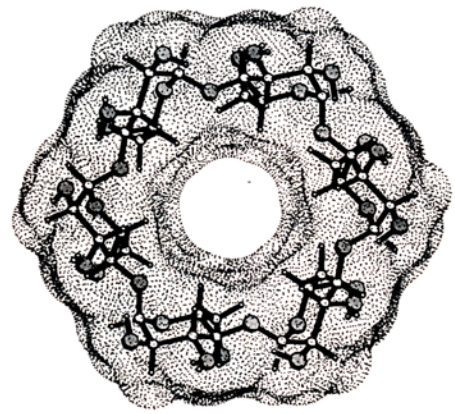

cyclo[D-Glc*p* α(1→4)]$_6$
4 (α-CD)

ably – in other positions of the pyranoid ring, e.g. at the anomeric carbon C-1. In considering this possibility, it becomes clear that bending of the pyranoid chair at C-1 would result in steric conflicts between the axial O-1, H-3, and H-5 atoms, and can only occur by an increase of two corresponding ring torsion angles ($C_2-C_1-O_5-C_5$ and $C_3-C_2-C_1-O_5$, respectively). Obviously, compensation of steric strain in pyranoid rings is energetically considerably more favorable through *diminution* of torsion angles than by their *enlargement*. This supposition receives support from the cyclogalactins evaluated in a recent modeling study[12]; in the all-*galacto* analogs of **3** and **4** – both glycosidic linkage positions within the pyranoid rings are inverted [→ β(1→4)-*galacto*, hence: "*inverso*-cyclodextrins"] – flattening occurs at C-1 when proceeding from the cyclogalactohexaoside to the respective pentamer, since here the two ring torsion angles involved can effect this by diminution of their values, rather than by their energetically less favored enlargement.

The origins of strain inherent in the cycloglucotrioside **1** are most distinctly articulated by MOLCAD program[25]-mediated color-coded projection of fragmental energetic contributions to the total strain energy (PIMM91[21]) onto ball-and-stick models[34] (Figure 3), wherein red colors indicate high-energy bending. In **1**, the glycosidic angle at O-1 ($\varphi \approx 123.5°$) is the most strained bond angle (Figure 3, left), an effect that is propagated to a minor extent towards C-2 and C-3 of the glucose units. The torsional strain energy centered around C-4 and C-5 (Figure 3, center) originates from large distortions of the pyranoid units towards the less stable E_1 conformation and bending of Θ_1 and Θ_2 (vide supra); torsion bending also affects the whole backbone of the macrocycle, including the intersaccharidic linkage (Φ and Ψ). The computed distortions originate mainly from close van der Waals contacts (Figure 3, right) between the axial H-5 atoms pointing towards the molecular center (H-5/H-5′ distances of approx. 1.91 Å only), which are minimized by energetically less costly bending of bond angles and torsions.

The rotamer population of the hydroxymethyl groups in relation to the pyranoid rings[35] is generally characterized such that of the three staggered conformations the *trans-gauche* (*tg*) form is the least favored due to 1,3-diaxial-like repulsions between O-4 and O-6[36–38]. None of the PIMM91 generated minimum-energy structures (Figure 2) contains such an unfavorable *tg* arrangement. Instead, for

Table 3. Conformation of the glucose units in relation to the number of pyranoid rings in the macrocycle: going from the cycloglucohexaoside **4**, via **3** and **2** to the cyclotrioside **1**, the ideal $^4C_1$ chair conformation is progressively bent towards E_1 envelope geometries by flattening at C-4 through decrease of the absolute values of the adjacent ring torsion angles $|\Theta_1|$ and $|\Theta_2|$. The steric strain and the geometrical requirements of the sugar units fitting into the small-ring structures is displayed by the overall kink angle ε for each glucose residue

Cyclodextrin	Mean geometry of pyranose units[a]	Kink angle[b] < ε >	Glucose conformation
cyclo[Glcα(1→4)]$_6$ (**4**, α-CD)	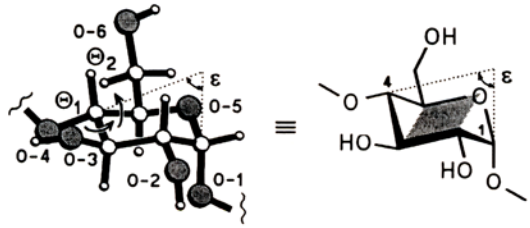	65.0±0.5°	$^4C_1$
cyclo[Glcα(1→4)]$_5$ (**3**)	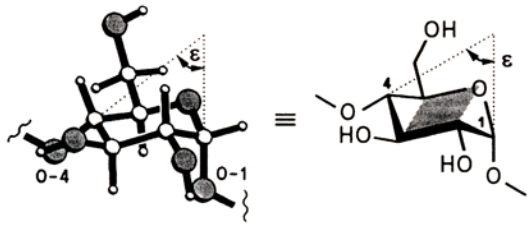	49.7±0.3°	$^4C_1$ (→ E_1)
cyclo[Glcα(1→4)]$_4$ (**2**)	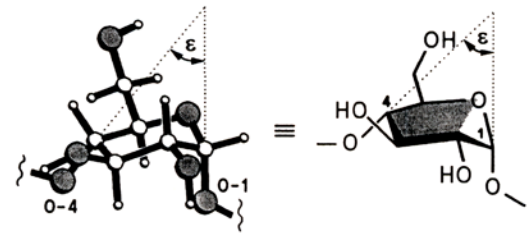	37.2±0.2°	E_1 (→ $^4C_1$)
cyclo[Glcα(1→4)]$_3$ (**1**)	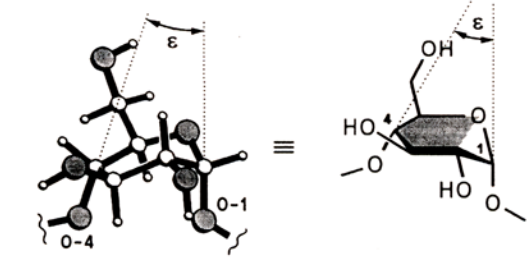	18.7±0.1°	E_1

[a] Global energy minimum structures found (PIMM91), oxygen atoms are shaded; the relevant ring planes are indicated in the conformational pictograms. – [b] Angle between the C_1-O_1 and C_4-O_4 bond vectors for each glucose residue.

α-cyclodextrin (**4**) and its small-ring analogs **1**–**3**, the *gauche-gauche* (*gg*) rotamers emerge as the most stable ones, whilst – most pronouncedly in the small-ring cyclodextrins **1** and **2** – the *gauche-trans* (*gt*) forms have considerably higher energies, respectively. In the *gt* form, the 6-CH_2OH groups point towards the center axis of the cyclodextrins, whilst the *gg* rotamers, directed towards the outside, are generally favored unless intermolecular hydrogen bonding with guest molecules included in the center cavity can take place[36].

The atomic distances from O-2 of one glucose unit to O-3 of the next, as listed in Table 2, reflect the geometrical constraints and pyranoid ring distortion on diminishing the number of glucose units as they become significantly larger: from ca. 3.1–3.3 Å in the hexamer (α-CD, **4**) and the pentamer **3**, i.e. prone to intramolecular hydrogen bonding of the 2-OH···O-3′-type, to ca. 3.8 Å for the tetramer **2** and as large as ca. 4.6 Å in the cycloglucotrioside **1**, both clearly devoid of such H-bond interactions. Indeed, for α-cyclodextrin (**4**) strong intramolecular hydrogen bonding was experimentally observed in solid-state structures[36,39] and in solution[40]; it not only explains the chemical inertness of the 3-OH groups[40], but also the high 2-*O*-selectivity of base-induced alkylations of α-cyclodextrin (**4**)[41], since the intermediate alkoxide anions are most efficiently stabilized via interresidue H-bonding in the 2-*O*-position[42,43].

High-Temperature Annealing of α-Cyclodextrin (4) and Cycloglucopentaoside 3

Inasmuch as symmetrical structures have been criticized not to represent the global minimum-energy conformations of cyclodextrins[23], we were induced to check the validity of our PIMM91[21]-derived results not only by another force-field – i.e. a modified CHARMM force-field specially adapted to carbohydrates[44] and successfully tested for glycol and cellulose[45] – but also by High-Temperature Annealing (HTA)[46], a methodology that exhaustively explores the whole accessible conformational space, and thus ensures all low-energy geometries to be seized provided the simulation time is long enough.

In HTA simulations[46], molecular structures are drawn in regular time steps from a high-temperature (1200 K) molecular dynamics (MD) trajectory and are slowly cooled down to 300 K to avoid ending up in irrelevant high energy minima. Subsequently, all structures obtained are fully energy-minimized by molecular mechanics (MM). The MD simulation allows Boltzmann-weighted averaging of all molecular parameters over the entire set of geometries in consideration of the total cyclodextrin energy; computed values are included in Table 2, and the global minimum-energy structures are shown in Figure 4.

The structural descriptors for the two cyclodextrins **3** and **4** differ significantly from those obtained from the PIMM91 analysis. Most notably, the tilt angles ($\tau \approx 85-90°$, cf. Table 2) indicate the glucose units to line up almost perpendicularly with respect to the macrocycle, with the 6-OH groups turned slightly towards the outside. As compared with the PIMM91-derived geometries, the changes in τ ($\Delta\tau \approx 10-20°$) account for the increase of Φ ($\rightarrow \approx 130°$), the decrease of Ψ ($\rightarrow \approx 110°$), and for the widening of the torus rim at the 6-OH side (enlargement of the average $C_6-C_{6'}$ distances from ≈4.3 Å to ≈5.2 Å) with concomitant contraction of the opposite aperture (mean $O_2-O_{3'}$ distances are reduced from ≈3.2 Å to ≈2.7 Å). This is obviously caused by an overestimation of hydrogen bonding energies between the 2-OH and 3′-OH groups of adjacent glucose units[47]. Accordingly, the HTA structures exhibit a less conical, but more cylindrical overall shape than the PIMM91 geometries. The *n*-polygon of all the O-1 atoms forms almost planar structures in **3** and **4** [calcd. root-mean-square atomic displacements from planarity ca. 0.05(4) Å and ca. 0.10(9) Å, respectively] and no significant puckerings for the entire macrocycles are computed.

When going from the α-cyclodextrin (**4**) to the pentamer **3**, slight flattening of the pyranose $^4C_1$ conformations at C-4 is indicated by an approximate 6° decrease of the ring torsion angles Θ_1 and Θ_2 and an increase of the Cremer-Pople puckering parameter θ ($\approx 15° \rightarrow \approx 21°$, with $\phi \approx 40-45°$, cf. Table 2). The puckering amplitude Q of approximately 0.61–0.62 Å may be slightly overestimated by the CHARMM force-field. It is noteworthy, that the calculated changes in Θ_1, Θ_2, and θ upon excision of one glucose unit from the macrocycle (**4** → **3**) are larger than the corresponding root-mean-square fluctuations, and thus are obviously significant.

Figure 3. Cyclo-α(1→4)-glucotrioside **1**: MOLCAD program generated representation of the fragmental energetic contributions of angle bending (left), dihedral distortions (center), and van der Waals interactions (right) to the total PIMM91 strain energy. For visualization, a 16-color code was used and projected onto a ball-and-stick model each, red colors corresponding to high internal strain energies, violet colors indicating unstrained molecular fragments

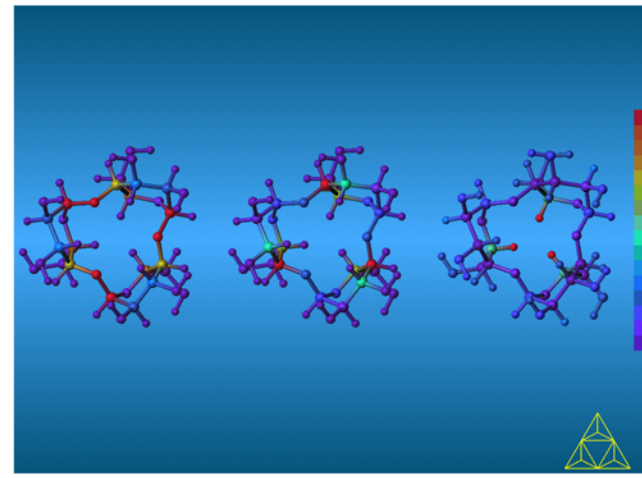

On the basis of multiple conformational transitions observed for the glucose units during the HTA simulation, the fully relaxed energy potential surfaces as a function of the pyranose puckering parameters Q, θ, and ϕ were calculated for the two cyclodextrins. The resulting three-dimensional isoenergy contour maps are plotted in polar coordinates (Figure 5, left), and their projections onto the equator plane are depicted alongside (Figure 5, right), allowing the total molecular energy of each cyclodextrin to be correlated with distinct conformations of the glucopyranose units.

In the case of α-cyclodextrin (**4**), a narrow and steep-contoured energy minimum close to the northern apex ($\theta \approx 10-15°$) of the $Q/\theta/\phi$-hypersuface of conformational states reveals almost unstrained $^4C_1$ geometries as the most stable conformations for the glucopyranose units. A shallow minimum barely below the +50 kJ/mol level in the $^1S_3$-skew (twist boat) region – i.e. distortion of at least one glucose residue towards a $^1S_3$ conformation increases the total molecular energy of **4** by approximately 50 kJ/mol – indicates

Figure 4. Molecular geometries of the high-temperature annealing derived global minimum-energy structures (modified CHARMM force-field) of cycloglucopentaoside (**3**, left) and α-cyclodextrin (**4**, right); the chosen mode of viewing is the same as in Figure 2

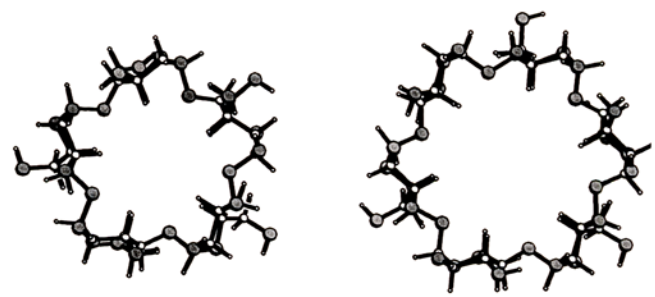

cyclo[D-Glc*p* α(1→4)]$_5$
3

cyclo[D-Glc*p* α(1→4)]$_6$
4 (α-CD)

Figure 5. Isoenergy contour surfaces of total molecular energies (HTA) as a function of the glucopyranose Cremer-Pople puckering parameters Q, θ, and ϕ for α-cyclodextrin (**4**) and its next lower homolog cyclo-α(1→4)-glucopentaoside (**3**). The polar coordinate plots at left signify a contour value of +50 kJ/mol above the global minimum; the circles in the 3D plots mark constant puckering amplitudes of $Q = 0.60$ and 0.80 Å. On the right, projections of the 3D energy contours onto the equator plane ($\theta = 90°$) are shown at relative +10, +25, and +50 kJ/mol levels (the global energy minimum is marked by an asterisk; circles correspond to puckerings of $Q = 0.60$ and 0.80 Å in the equator plane for $\theta = 90°$). In addition, the relevant glucopyranose conformations are inserted as pictograms

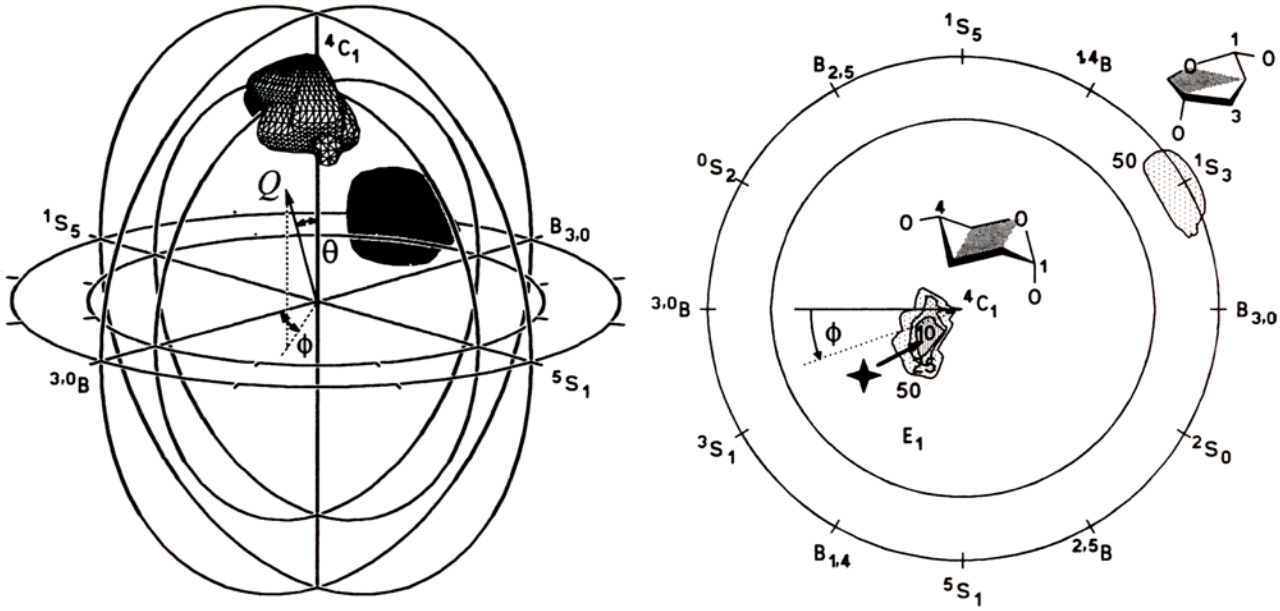

cyclo[D-Glc*p* α(1→4)]$_6$
4 (α-CD)

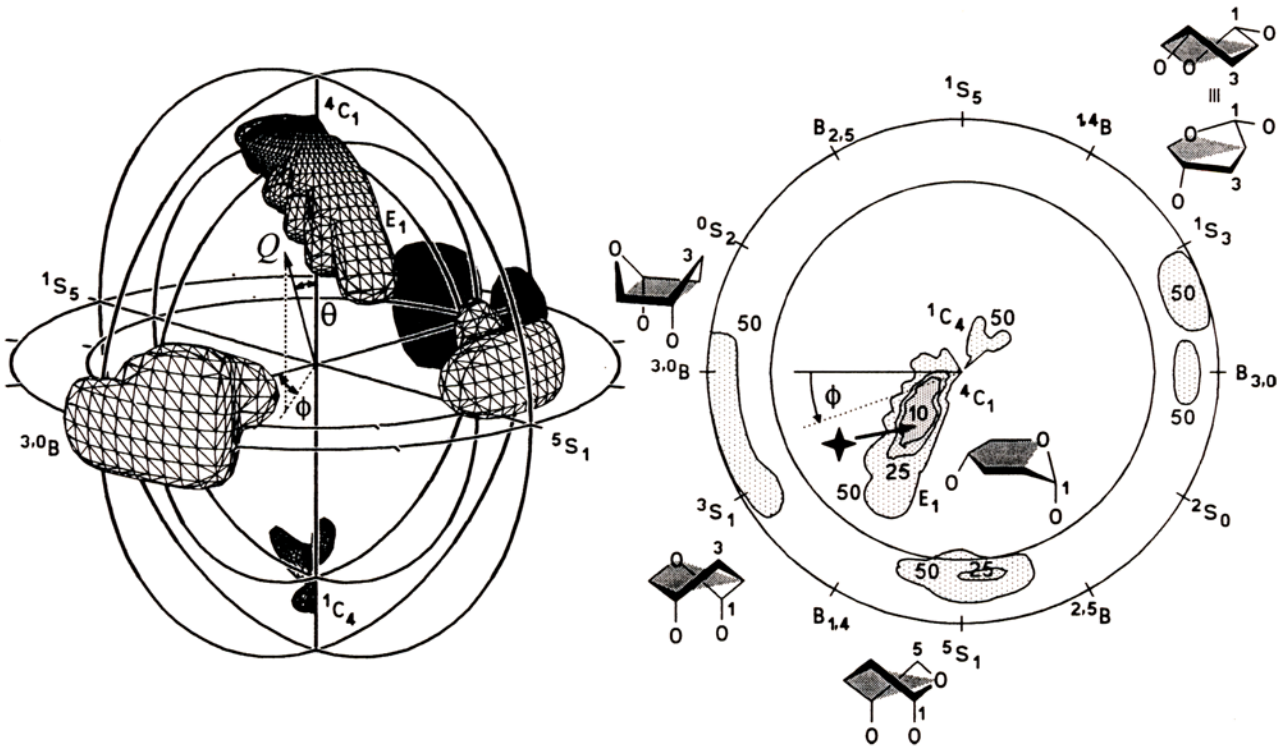

cyclo[D-Glc*p* α(1→4)]$_5$
3

that distorted pyranose conformations will be adopted only if α-cyclodextrin is perturbed by strong forces such as, for example, strong interactions with encapsulated guest molecules[48].

Figure 6. Cross section plots of a plane perpendicular to the macrocycle mean plane with the contact surfaces of the cyclodextrins **1**–**4**. Contours were obtained for successive 10° rotation steps around the geometrical center M and superimposed. In each case, the widely opened torus rim of the secondary 2-OH/3-OH groups is on top, and the narrow aperture made up by the primary 6-OH groups on the bottom side; approximate molecular dimensions are included

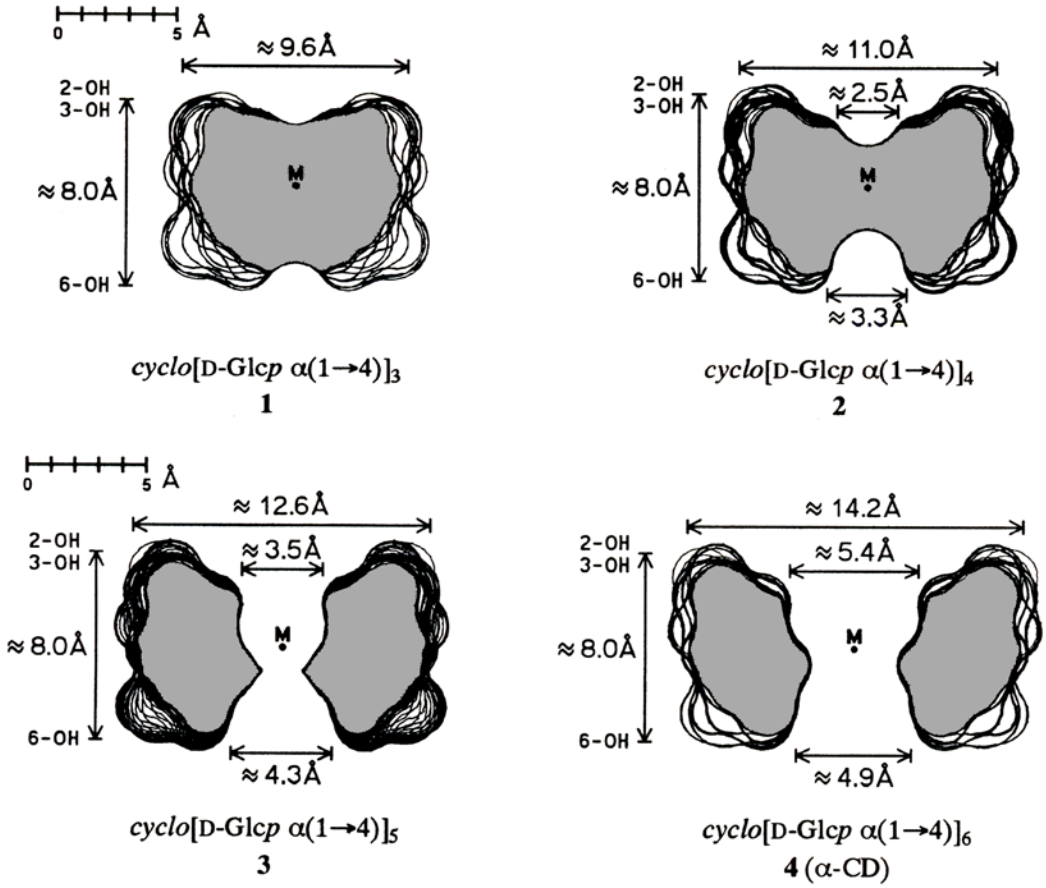

cyclo[D-Glc*p* α(1→4)]$_3$ **1**

cyclo[D-Glc*p* α(1→4)]$_4$ **2**

cyclo[D-Glc*p* α(1→4)]$_5$ **3**

cyclo[D-Glc*p* α(1→4)]$_6$ **4** (α-CD)

Table 4. Molecular dimensions and cavity characteristics of cyclodextrins **1**–**6** (PIMM91 structures)

Cyclodextrin		Torus Ø [Å] outer	inner	Torus height	Surface area [Å^2] total	cavity	Molecular volume [Å^3] total	cavity	exp.[a]
6	γ-CD	17.3	8.4	8.0	960	140	1305	250	1330
5	β-CD	15.7	6.6	8.0	845	105	1140	160	1168
4	α-CD	14.2	5.2	8.0	720	85	975	100	1010
3		12.6	3.9	8.0	605	60	815	50	–
2		11.0	(3.0)[b]	8.0	475	(15)[b]	660	(5)[b]	–
1		9.6	–	8.0	370	–	495	–	–

[a] Apparent molar volume $^{\Phi}V$ for dilute aqueous solutions[51]. – [b] Surface dent only, no cavity.

For the cycloglucopentaoside **3**, the global energy minimum for the pyranose conformations (Figure 5) is still located close to the north pole ($^4C_1$), albeit the energy contours become significantly smoother and more extended than in **4**, and are slightly shifted to larger latitudes (increasing θ) in the direction towards E_1 geometries ($\phi \approx 45°$, cf. Table 2). Additional local energy minima of ca. +25 kJ/mol in the $^5S_1$ region, and ca. +50 kJ/mol for $^{3,O}B \leftrightarrow {}^3S_1$, $B_{3,O} \leftrightarrow {}^1S_3$, and inverted $^1C_4$ conformations, indicate that alternate pyranose conformations are energetically more readily accessible in the pentamer **3** than in α-cyclodextrin (**4**). Obviously, the strain inherent in **3** results in a tendency of both the C_1-O_1 and the C_4-O_4 bonds to adopt pseudo-axial orientations that enable alternate pyranose geometries through release of strain from the macrocycle.

By the way of summation, the conformational properties of the glucopyranose units in **3** and **4** that emerged from the PIMM91 calculations (cf. Table 1) are fully substantiated

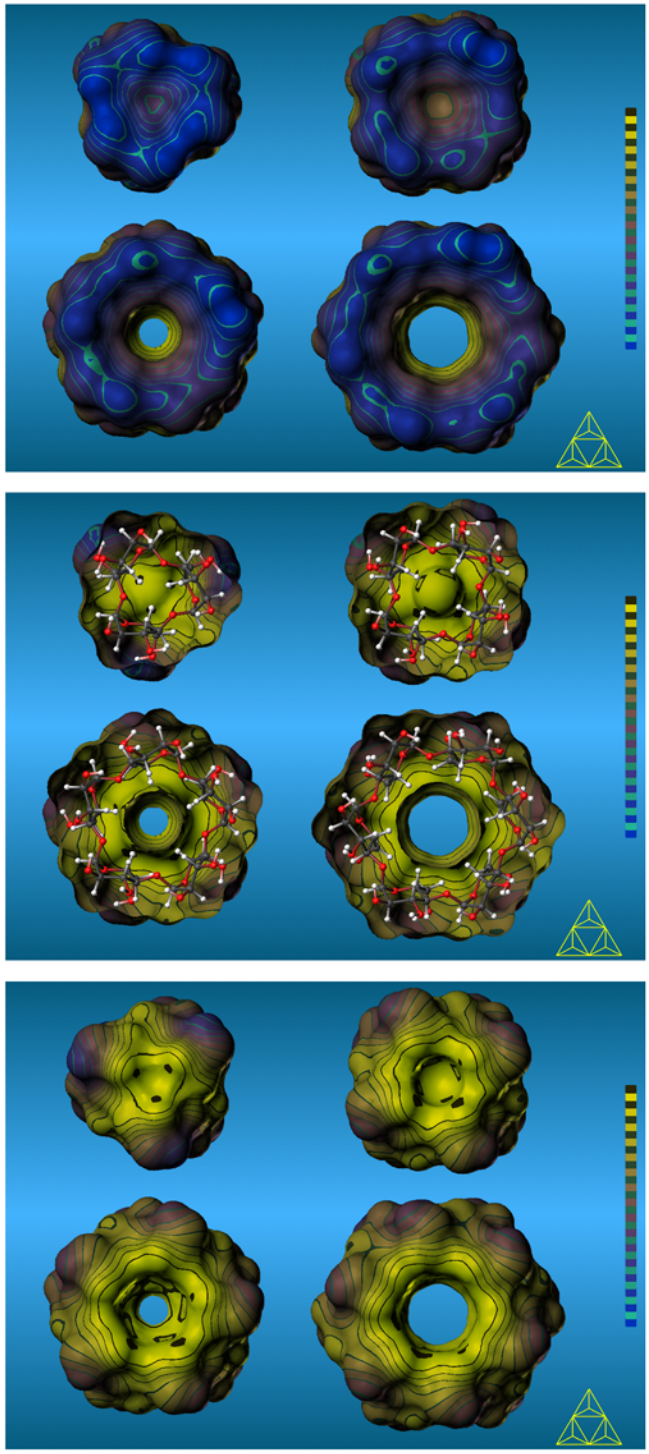

Figure 7. MOLCAD program generated molecular lipophilicity patterns (MLP) projected onto the contact surfaces of *cyclo*[Glcα(1→4)]$_3$ (**1**, upper left), *cyclo*[Glcα(1→4)]$_4$ (**2**, upper right), *cyclo*[Glcα(1→4)]$_5$ (**3**, lower left), and *cyclo*[Glcα(1→4)]$_6$ (**4**, α-CD, lower right). For visualization a two-color code graded into 32 shades is used. The color coding was adapted to the range of relative hydrophobicity calculated for each molecule, by using 16 colors ranging from dark blue (most hydrophilic surface areas) over light blue to full yellow (most hydrophobic regions) for mapping the computed values onto the surface. The remaining 16 color shades (light blue to brown) were used to indicate isocontour lines in between former color scale, allowing a more quantitative assessment of relative hydrophobicity on different surface regions. The *top* picture views through the larger openings of the conically shaped molecules, thus exposing the intensively hydrophilic (blue) 2-OH/3-OH side. In the *middle*, the hydrophilic front half of the surface has been removed providing an inside view onto the hydrophobic (yellow) backside; in addition, a ball-and-stick model was inserted to illustrate the molecular orientation (mode of viewing analog to Figure 2). The *bottom* representation depicts the "backside" of the cyclodextrins (i.e. the smaller opening with the 6-CH_2OH groups facing the viewer), clearly exposing the hydrophobic (yellow) surface areas, that in the case of **3** and **4** extend well into the cavity

by the HTA data, particularly with respect to the distinct progressive flattening of the pyranose units at C-4 on reduction of the ring size. However, the PIMM91 structures (cf. Figure 2) exhibit molecular parameters closest to the corresponding experimental expectation values, most notably, the glucose tiltings are properly reproduced. In addition, these symmetrical geometries represent the best molecular pictures for the time-averaged overall shapes of the cyclodextrins **1**–**4**, and thus are used in the sequel to further evaluate their physico-chemical properties.

Cyclodextrin Contact Surfaces and Cavity Dimensions

Already the cyclodextrin $O_1-O_{1'}$ distances listed in Table 2 sustain the notion that of the small-ring cyclodextrins only the pentamer **3** is to exhibit a central cavity large enough to include small guest molecules. To further assess this, the contact surfaces[26] – closely related to the solvent-accessible surfaces[49] – were generated by the MOLCAD program[25] and depicted in dotted form (Figure 2). For better visualization of the extension of these surfaces and the cavity proportions, cross cuts through the contact surfaces were calculated and the respective contour lines originating from successive 10° rotation around the geometrical center M were superimposed (Figure 6). The effective molecular dimensions displayed by these surface cuts are listed in Table 4 and compared to those of the higher cyclodextrin homologs β-cyclodextrin (**5**) and γ-cyclodextrin (**6**).

In essence, the well-established conical doughnut shape of the native cyclodextrins **4**–**6** is retained in the smaller analogs **1**–**3**, with the wide-opened rim of the torus being made up by the 2-OH and 3-OH groups, the narrower aperture carrying the 6-CH_2OH groups. The respective tori exhibit essentially constant heights of approximately 8 Å (cf. Figure 6). As is also clearly evident, the pentameric cyclodextrin **3** features a cavity similar, yet distinctly smaller than the α-cyclodextrin (**4**), the inner diameter being less than 4 Å. In the tetrameric homolog **2**, and in the trimer **1**, there is no cavity at all: **2** exhibits a substantial indentation on the top and bottom sides of the cone (Figure 6), whereas **1** features only a shallow surface dent, and thus resembles more closely a solid frustum rather than a torus.

The cavity interior comprises approximately 10–15% of the total cyclodextrin surface area (Table 4, ≈120 Å^2/glucose unit)[50]. The spatial volume included by the contact surfaces closely corresponds to the apparent molar volume $^{\phi}V$ required by these compounds in aqueous solution. The conformity of the values calculated for the native cyclodextrins **4**–**6** (Table 4, ≈160–165 Å^3/glucose unit) with the volumes obtained from density measurements in aqueous solution[51] indicates the central hole to be occupied by

Figure 8. Side view MLPs, in closed and bisected form each, of the four α(1→4)-cyclodextrins **1**−**4** with three (**1**, upper left), four (**2**, upper right), five (**3**, lower left), and six (**4**, α-CD, lower right) glucose units, respectively; color coding according to Figure 7. Their orientation is uniformly such that the 2-OH/3-OH side is aligned upward (larger opening of the torus) and the 6-CH_2OH points downward (smaller aperture). The similarities in the distribution of hydrophilic (blue) and hydrophobic surface areas − most notably on the inside regions of the cavities of **3** and **4** (upper rows, each) − are clearly apparent

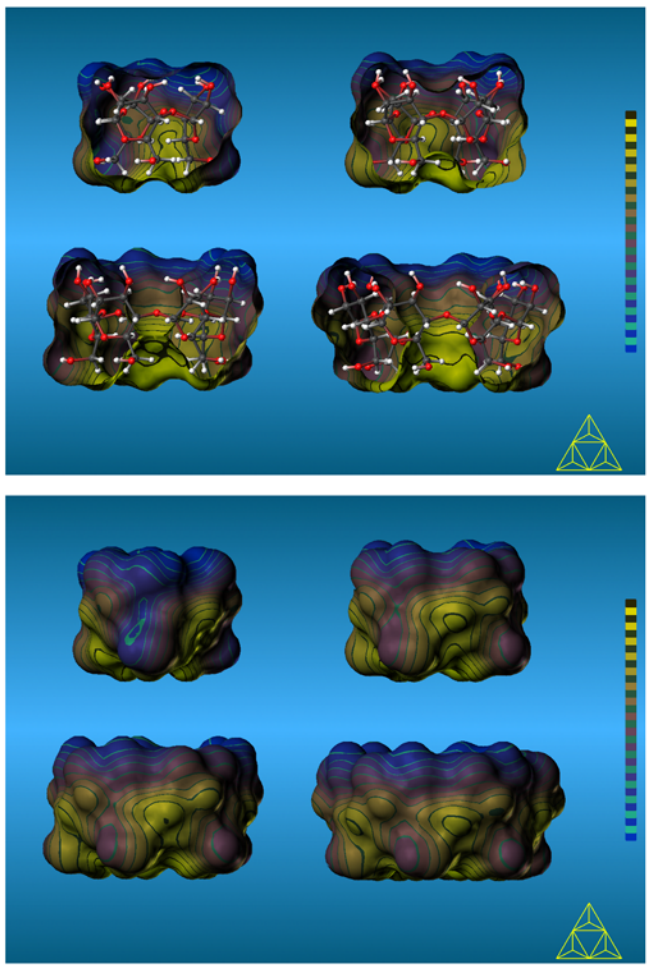

water molecules; otherwise, much larger apparent volumes would have to be observed. In the case of α-cyclodextrin hexahydrate, crystal structural data[22] revealed an asymmetrically distorted cavity of approx. 5 Å width and a volume of ca. 100 Å^3[50], able to accommodate two water molecules ($^{\Phi}V_{H_2O} \approx 30$ Å^3) in well-defined positions. The high-pressure inclusion of krypton − with its van der Waals diameter of ca. 4.0 Å krypton is comparable in size to a water molecule − leads to a less distorted α-cyclodextrin solid-state structure, in which krypton only fits loosely the cavity with a statistical positional distribution[52]. The comparison of both the water and krypton inclusion complexes of α-cyclodextrin clearly indicates the flexibility of the cavity for adopting towards different guest molecules[52].

From the cavity volume of approx. 50 Å^3 calculated for the cyclopentaoside **3**, it may be inferred that it should exhibit complexing capabilities for at least small molecules, provided that the pocket also exhibits a certain degree of flexibility. The noble gases krypton (van der Waals radius ≈1.9 Å), argon ($r_{VDW} \approx 1.8$ Å), and neon ($r_{VDW} \approx 1.5$ Å) might fit into the cavity, as well as one molecule of water. The latter hypothesis should be the most easiest to be verified: comparison of the experimental apparent molar volume determined by simple density measurements of aqueous solutions of **3** and comparison with the calculated volume of ca. 815 Å^3 (Table 4) may result in a direct proof for inclusion of water.

Molecular Lipophilicity Patterns of Cyclodextrins 1−4

Aside from the imperative fulfilment of steric requirements, the hydrophobic effect[53] represents the most important factor in governing guest-host interactions in the cyclodextrin series[2]. Concomitantly, the release of complexed water from the cyclodextrin cave and the hydrophobic hydration sphere[53] of the guest to be incorporated into the bulk aqueous phase must be considered as the main entropic factor favoring complex formation. However, this favorable contribution to entropy is usually over-compensated by the loss of degrees of freedom from combining two independent molecules into one complex and the complexation by cyclodextrins is enthalpically driven in most cases[54].

The color-coded visualization of **m**olecular **l**ipophilicity **p**atterns (MLP)[55] projected onto molecular contact surfaces by using the MOLCAD molecular modeling program[25,56] is especially suited for the assessment of hydrophobic interactions[57]. The MLPs for the four cyclooligosaccharides **1**−**4** are depicted in Figs. 7 and 8 in a two-color code graded into 32 shades, ranging from dark blue for the most hydrophilic areas to yellow for the most hydrophobic regions.

The lipophilicity patterns of the cyclodextrins reveal the 2-OH/3-OH side of the macrocycles, i.e. the respective wider torus rim, to be distinctly hydrophilic, as evidenced by the clearly defined blue areas (Figure 7, top). This is contrasted with the intensely hydrophobic (yellow) surface regions on the opposite side − the narrower opening made up by the 6-CH_2OH groups − which in the case of α-cyclodextrin (**4**) and the pentamer **3** extend well into the cavity. For the smaller cyclodextrins **1** and **2**, devoid of a cavity, the respective center identation (**2**) and the shallow surface dent (**1**) are the most hydrophobic regions. An even more articulate impression of the MLPs is provided by the juxtaposition of the respective side views in closed and half-opened form (Figure 8).

Accordingly, the cycloglucopentaoside **3** is surmised not only to be capable of inclusion of small molecules on geometrical grounds, but also on the basis of its hydrophobicity characteristics, which closely resemble those of α-cyclodextrin (**4**); only the narrower cavity substantially limits the type of molecules to form inclusion complexes − methanol, methan, carbon dioxide, and the noble gases being adequate candidates in terms of geometry and hydrophobic interactions. The two smaller cyclodextrins **1** and **2** − if

ever synthesized – should exhibit binding of hydrophobic molecules in a sandwich type manner only.

Conclusions

The molecular modelings presented clearly provide a concise picture of cyclodextrin features – in terms of their geometrical and conformational properties as well as their molecular lipophilicity patterns – as a function of their ring size. Some properties well-established for α-cyclodextrin (**4**) are uniformly maintained throughout the entire series of small-ring cyclodextrins **1**–**3**, i.e. the tilting of the glucose units in respect of the macrocycle, for example, whilst others, most notably the puckering of the pyranose units, change substantially in the smaller homologs. On the basis of the calculatory data, the proposition of large steric strains to be responsible for the absence of at least the "unnatural" cyclopentaoside **3** in the enzymatic digestions of starch has to be discarded. However, the increasing strain energy in **2** and finally **1**, has far-reaching implications on the chances of these compounds ever to be synthesized being rather dim, but not entirely illusive.

Contraction of the cyclodextrins by successive excision of one glucose unit from the ring expresses itself most significantly in a clear narrowing of the central cavity, the cycloglucotetraoside **2** and the trioside **1** even lacking a hole penetrating the macrocycle. The hydrophobicity pattern of the pentamer **3** resembles closely that of the native α-cyclodextrin (**4**) and consequently must lead to the conclusion, that the largest of the small-ring cyclodextrins should be capable of forming inclusion complexes with small molecules of appropriate dimensions. In contrast to this, the homologs **2** and **1** should be amenable to hydrophobic binding via their surface indentation only, so that the formation of inclusion complexes is expected to be impossible.

Experimental

Glucose Tilt Angle τ Variations: For the generation of the structures of the native α-cyclodextrin (**4**) and its small-ring analogs **1**–**3**, PIMM91 geometry-optimized glucose $^4C_1$ conformations exhibiting different hydroxymethyl torsions (*gg*, ω = −60°, and *gt*, ω = +60°) were assembled to form symmetrical structures (i.e. all $O_1/O_{4'}$ atoms forming a regular *n*-polygon) by using a rigid body rotation and fitting procedure[58]; thereby the glucose tilt angles τ were varied in the range from +60 to +140° in steps of 5°. After geometrical repositioning of all CH and OH hydrogen atoms, avoiding close steric contacts and considering different hydroxyl group torsions, each structure was fully optimized without any restraints by using the PIMM91 force-field program[21] for in vacuo conditions (ε = 1); the resulting global minimum-energy structures given in Figure 2 were used for the generation of the contact surfaces and molecular lipophilicity patterns.

HTA Calculations: For determination of the lowest molecular energy conformations of the pentamer **3** and the hexameric α-cyclodextrin (**4**) by high-temperature annealing (HTA)[46], a modified force-field specially adapted for carbohydrates[44,45] was used. The Verlet integrator[59] was applied in the MD simulation program CHARMM[60] with a time step of 1 fs at constant temperature[61] and a dielectric constant ε = 1. Out of MD trajectories at 1200 K (4382 ps for **3**, 2000 ps for **4**) every 1000 fs the respective conformation was allowed to cool down to 300 K at a rate of 10 K/fs, was held there for additional 1010 fs, and subsequently fully energy-minimized by an adapted Newton-Raphson algorithm of the CHARMM22 program package[60] with a convergence criterion of 10^{-7} kcal/mol.

In the case of the cycloglucopentaoside **3**, a total of 3264 (75%) different conformers (corresponding to 16320 glucose units) were entered into geometry analysis, in the case of α-cyclodextrin (**4**) total of 1675 (84%) structures (10050 glucose residues) were used. All molecular parameters and root-mean-square (RMS) deviations were determined by Boltzmann-weighted averaging (300 K) by using the total cyclodextrin energies.

Energy Potential Surfaces and Contour Plots: For computation of the cyclodextrin energy potential surface as a function the Cremer-Pople parameters[28,29], the HTA data set $\Delta H_f^{298} = f(Q, \theta, \phi)$ of **3** and **4** was divided into classes $[Q + \Delta Q, \theta + \Delta\theta, \phi + \Delta\phi]$ for the 3D plot (Figure 5, $\Delta H_{rel} \approx 0$–230 kJ/mol, 0.52 Å $\leq Q \leq$ 0.84 Å, 0° $\leq \theta \leq$ 180°, and 0° $\leq \phi \leq$ 360°, width of classes ΔQ = 0.05 Å and $\Delta\theta = \Delta\phi$ = 10°) and classes $[Q \sin\theta, \phi]$ for 2D contouring (window size $\Delta(Q \sin\theta)$ = 0.05 Å and $\Delta\phi$ = 10°). For each class, energies were Boltzmann-averaged (300 K); the contour plots were computed by using cubic regression formulas and plotted in polar coordinates.

Molecular Surfaces and Molecular Lipophilicity Patterns: Calculation of the molecular contact surfaces and MLPs was carried out by using the MOLCAD[25] molecular modeling program and texture mapping[56]; a detailed description of the computational basics is given by Brickmann et al.[55] Scaling of the hydrophobicity profiles was performed in arbitrary units and in relative terms for each molecule separately, and no absolute values are displayed (no significant differences are observed by applying absolute overall scaling). Color graphics were photographed from the computer screen of a SILICON-GRAPHICS workstation.

☆ This account is dedicated to *Friedrich Cramer*, one of the pioneers in the exploration of cyclodextrins[2a].

[1] Part 5: F. W. Lichtenthaler, S. Immel, *Int. Sugar J.* **1995**, *97*, 12–22.

[2] [2a] F. Cramer, *Einschlussverbindungen*, Springer-Verlag, Berlin/Heidelberg, **1954**. – [2b] W. Saenger, *Angew. Chem.* **1980**, *92*, 343–361; *Angew. Chem. Int. Ed. Engl.* **1980**, *19*, 344–362. – [2c] G. Wenz, *Angew. Chem.* **1994**, *106*, 851–870; *Angew. Chem. Int. Ed. Engl.* **1994**, *33*, 803–822.

[3] K. Harata, *Recent Advances in the X-Ray Analysis of Cyclodextrin Complexes*, in: *Inclusion Compounds* (Eds.: J. L. Atwood, J. E. D. Davies, D. D. MacNicol), Oxford Univ. Press, Oxford, Vol. 5, **1991**, pp. 311–344.

[4] T. Fujiwara, N. Tanaka, S. Kobayashi, *Chem. Lett.* **1990**, 739–742.

[5] D. French, *Adv. Carbohydr. Chem.* **1957**, *12*, 189–260.

[6] A. O. Pulley, D. French, *Biochem. Biophys. Res. Commun.* **1961**, *5*, 11–15.

[7] P. R. Sundararajan, V. S. R. Rao, *Carbohydr. Res.* **1970**, *13*, 351–358.

[8] D. Duchene, D. Wouessidjewe, *J. Coord. Chem.* **1992**, *27*, 223–236.

[9] T. Nakagawa, K. Ueno, M. Kashiwa, J. Watanabe, *Tetrahedron Lett.* **1994**, *35*, 1921–1924.

[10] M. Mori, Dissertation, Univ. of Tokyo, **1991**; mentioned in ref.[11]

[11] H. Kuyama, T. Nukada, Y. Nakahara, T. Ogawa, *Tetrahedron Lett.* **1993**, *34*, 2171–2174.

[12] F. W. Lichtenthaler, S. Immel, *Tetrahedron Asymmetry* **1994**, *5*, 2045–2060.

[13] *Cyclodextrin News* (Ed.: J. Szejtli), Cyclolab FDS Publ., Budapest, **1994**, *9*, 41–42.

[14] Abbreviated Terminology of Oligosaccharide Chains, *J. Biol.*

Chem. **1982**, *257*, 3352–3354; *Pure Appl. Chem.* **1982**, *54*, 1523–1526.

[15] S. Houdier, P. J. A. Vottéro, *Angew. Chem.* **1994**, *106*, 365–367; *Angew. Chem. Int. Ed. Engl.* **1994**, *33*, 354–356.

[16] P. M. Collins, M. H. Ali, *Tetrahedron Lett.* **1990**, *31*, 4517–4520.

[17] M. Mori, Y. Ito, T. Ogawa, *Tetrahedron Lett.* **1989**, *30*, 1273–1276; *Carbohydr. Res.* **1989**, *192*, 131–146.

[18] The epoxide ring in a β-cyclodextrin carrying one 2,3-anhydromannose unit can smoothly be opened by refluxing in water to give a cyclooligosaccharide with one altrose and six glucose residues, i.e. *cyclo*{D-Alt*p*α(1→4)-[D-Glc*p*α(1→4)]$_6$} (cf. K. Fujita, K. Ohta, Y. Ikegami, H. Shimada, T. Tahara, Y. Nogami, T. Koga, K. Saito, T. Nakajima, *Tetrahedron Lett.* **1994**, *35*, 9577–9580). Application of the same simple conditions to the known per-2,3-anhydro-β-cyclomannin (A. R. Khan, L. Barton, V. T. D'Souza, *J. Chem. Soc., Chem. Commun.* **1992**, 1112–1114) are apt to yield the β-cycloaltrin.

[19] [19a] M. Kawamura, T. Uchiyama, T. Kuramoto, Y. Tamura, K. Mizutani, *Carbohydr. Res.* **1989**, *192*, 83–90. – [19b] M. Sawada, T. Tanaka, Y. Takai, T. Hanafusa, T. Taniguchi, M. Kawamura, T. Uchiyama, *Carbohydr. Res.* **1991**, *217*, 7–17.

[20] We prefer the tilt angle τ to the alternative angle τ′ (cf. ref.[3]) between the cyclodextrin mean plane and the best-fit plane of O_1, C_1, C_4, and O_4 of each glucose residue, since τ directly correlates with the nearly perpendicular orientation of the glucose units toward the macrocyclic ring; yet $\tau \approx \tau' + 90°$. Values of τ larger than 90° correspond to a rotation of the glucose moiety its O-6 side towards the molecular center.

[21] [21a] H. J. Lindner, *Closed Shell PI-SCF-LCAO-MO-Molecular Mechanics Program (PIMM91)*, Technische Hochschule Darmstadt, **1988**. – [21b] A. E. Smith, H. J. Lindner, *J. Comput.-Aided Mol. Des.* **1991**, *5*, 235–262.

[22] [22a] P. C. Manor, W. Saenger, *J. Am. Chem. Soc.* **1974**, *96*, 3630–3639. – [22b] W. Saenger, *Nature* **1979**, *279*, 343–344. – [22c] B. Klar, B. E. Hingerty, W. Saenger, *Acta Crystallogr., Sect. B*, **1980**, *36*, 1154–1165. – [22d] K. Lindner, W. Saenger, *Acta Crystallogr., Sect. B*, **1982**, *38*, 203–210. – [22e] K. K. Chacko, W. Saenger, *J. Am. Chem. Soc.* **1981**, *103*, 1708–1715.

[23] [23a] H. Dodziuk, K. Nowinski, *J. Mol. Struc. (THEOCHEM)* **1994**, *110*, 61–68. – [23b] K. B. Lipkowitz, *J. Org. Chem.* **1991**, *97*, 6357–6367.

[24] J. E. H. Koehler, W. Saenger, W. F. van Gunsteren, *Eur. Biophys. J.* **1987**, *15*, 197–210; *J. Mol. Biol.* **1988**, *203*, 241–250; *J. Biomol. Struc. Dyn.* **1988**, *6*, 182–198.

[25] [25a] J. Brickmann, *MOLCAD – MOLecular Computer Aided Design*, Technische Hochschule Darmstadt, **1992**. The major part of the MOLCAD program is included in the SYBYL package of TRIPOS Associates, St. Louis, USA. – [25b] J. Brickmann, *J. Chim. Phys.* **1992**, *89*, 1709–1721. – [25c] M. Waldherr-Teschner, T. Goetze, W. Heiden, M. Knoblauch, H. Vollhardt, J. Brickmann, in: *Advances in Scientific Visualization* (Eds.: F. H. Post, A. J. S. Hin), Springer Verlag, Heidelberg, **1992**, pp. 58–67. – [25d] J. Brickmann, T. Goetze, W. Heiden, G. Moeckel, S. Reiling, H. Vollhardt, C.-D. Zachmann, *Interactive Visualization of Molecular Scenarios with MOLCAD/SYBYL, in: Insight and Innovation in Data Visualization* (Ed.: J. E. Bowie), Manning Publications Co., Greenwich, **1994**, pp. 83–97.

[26] [26a] F. M. Richards, *Ann. Rev. Biophys. Bioeng.* **1977**, *6*, 151–176; *Carlsberg. Res. Commun.* **1979**, *44*, 47–63. – [26b] M. L. Connolly, *J. Appl. Cryst.* **1983**, *16*, 548–558; *Science* **1983**, *221*, 709–713.

[27] C. Morat, F. R. Taravel, *Bull. Magn. Res.* **1989**, *11*, 321–323; *Tetrahedron Lett.* **1990**, *31*, 1413–1416.

[28] D. Cremer, J. A. Pople, *J. Am. Chem. Soc.* **1975**, *97*, 1354–1358.

[29] G. A. Jeffrey, J. H. Yates, *Carbohydr. Res.* **1979**, *74*, 319–322.

[30] For six-membered rings three polar coordinate-type Cremer-Pople (CP) parameters[28,29] Q, θ, and φ are necessary to describe the ring conformation. The puckering amplitude Q serves as a measure of the ring distortion only, being related to a mean-square atomic deviation from planarity. The angles θ (latitude) and φ (longitude) describe the ring conformation, e.g. $\theta \approx 54.7°/\phi \approx 60.0°$ corresponds to an E_1 geometry, while $\theta \approx 0.0°$ (in polar coordinates φ becomes meaningless for $\theta \rightarrow 0°$) is found for $^4C_1$ geometries.

[31] [31a] *Cambridge Crystallographic Data File*, Version 5.04, **1993**, data sets with missing coordinates and more recent structure determinations have been included if atomic coordinates are provided within the written publications. – [31b] F. H. Allen, S. A. Bellard, M. D. Brice, B. A. Cartwright, A. Doubleday, H. Higgs, T. Hummelink, B. G. Hummelink-Peters, O. Kennard, W. D. S. Motherwell, J. R. Rodgers, D. G. Watson, *Acta Crystallogr., Sect. B* **1979**, *35*, 2331–2339. – [31c] F. H. Allen, O. Kennard, R. Taylor, *Acc. Chem. Res.* **1983**, *16*, 146–153.

[32] The solid-state structures of different crystal forms of non-complexed α-cyclodextrin (**4**)[22] revealed asymmetric distortions, which are not retained in (aqueous) solution[24]. For statistical reasons, and in order to obtain a general overview of the conformational features of **4**, its inclusion complexes were included into the geometry analysis.

[33] Experimental proof for the slight flattening at C-4 in **3** may be derived from the ^{1}H-^{1}H-NMR coupling constants of its peracetate synthesized recently[9], which with $J_{3,4} \approx 7.6$ and $J_{4,5} \approx 8.3$ Hz are smaller than those usually found in the cyclodextrins ($J_{3,4} \approx J_{4,5} \approx 9.0–9.5$ Hz, cf. A. F. Casy, A. D. Mercer, *Magn. Res. Chem.* **1988**, *26*, 765–774).

[34] H. Vollhardt, Diploma Thesis, Technische Hochschule Darmstadt, **1991**.

[35] The orientation of the hydroxymethyl group is defined by two torsion angles $O_5–C_5–C_6–O_6$ (≡ ω) and $C_4–C_5–C_6–O_6$. In principle, the ω angle can have any value in the −180° to +180° range, but generally the conformations to be considered are the three staggered ones, referred to as *gg*, *gt*, and *tg* forms, wherein the first letter denotes the orientation of O-6 towards the pyranoid ring oxygen.

[36] G. A. Jeffrey, W. Saenger, *Hydrogen Bonding in Biological Structures*, Springer Verlag, Berlin/New York, **1991**; or particular relevance in this context is Chapter 18: *OH···O Hydrogen Bonding in Crystal Structures of Cyclic and Linear Oligoamyloses: Cyclodextrins, Maltotriose, and Maltohexaose*, pp. 309–350; most notably pp. 315–318.

[37] L. M. J. Kroon-Batenburg, J. Kroon, *Biopolymers* **1990**, *29*, 1243–1248.

[38] K. Bock, J. Ø. Duus, *J. Carbohydr. Chem.* **1994**, *13*, 513–543.

[39] T. Steiner, W. Saenger, *Carbohydr. Res.* **1994**, *259*, 1–12.

[40] B. Casu, M. Reggiani, G. G. Gallo, A. Vigevani, *Tetrahedron* **1968**, *24*, 803–821.

[41] D. Rong, V. T. D'Souza, *Tetrahedron Lett.* **1990**, *31*, 4275–4278.

[42] See ref.[36], Chapter 13: *Hydrogen Bonding in Carbohydrates*, pp. 169–219; most notably pp. 183–185 and 198.

[43] F. W. Lichtenthaler, S. Immel, D. Martin, V. Müller, *Starch/Stärke* **1992**, *44*, 445–456.

[44] S. Reiling, M. Schlenkrich, J. Brickmann, *J. Comput. Chem.* **1995**, in press.

[45] [45a] S. Reiling, M. Schlenkrich, P. A. Bopp, J. Brickmann, *J. Comput. Chem.* **1995**, in press. – [45b] S. Reiling, J. Brickmann, *Macromol. Chem. (Theory and Simulations)* **1995**, in press.

[46] A. T. Brünger, *Annu. Rev. Phys. Chem.* **1991**, *42*, 197–205.

[47] In both force-fields, hydrogen bonding is treated exclusively as an electrostatic interaction, no special energy terms are added to account for H-bonds. The significantly higher charges of the modified CHARMM force-field[44] (approx. atomic charges of −OH: −0.66 and +0.43, acetal oxygens −0.36, carbon +0.14, and ring protons +0.09) in contrast to PIMM91[21] (partial charges of all oxygens −0.32 to −0.35, carbon +0.10 to +0.20, hydroxyl-H +0.20, and C-H +0.00 to +0.10) lead to higher H-bond interaction energies in the former.

[48] A reliable proof of a guest-induced conformational transition of a pyranose ring system was found in the solid-state structure of the heptakis(2,3,6,-tri-*O*-methyl)-β-cyclodextrin *m*-iodo phenol inclusion complex (K. Harata, F. Hirayama, H. Arima, K. Uekama, T. Miyaji, *J. Chem. Soc., Perkin Trans. 2*, **1992**, 1159–1166), with one glucose residue adopting a $^OS_2$ conformation (recalcd. $Q = 0.722$ Å, $\theta = 86.7°$, and $\phi = 323.6°$). The distorted ^2E (→ ^{2,5}B) glucose conformation in an α-cyclodextrin structure (B. Klingert, G. Rihs, *J. Chem. Soc., Dalton Trans.* **1991**, 2749–2760) might originate from an error in the atomic coordinates (recalc. $Q = 0.538$ Å, $\theta = 68.0°$, and $\phi = 114.9°$).

[49] B. Lee, F. M. Richards, *J. Mol. Biol.* **1971**, *55*, 379–400.

[50] Mathematical definition of the cavity dimensions and volumens: cross section cuts of the cyclodextrin contact surface with planes parallel to the mean plane of the macrocycle (*x*/*y*-plane) were calculated in steps of $\Delta z = 0.05$ Å. The topmost and bottommost contours exhibiting separate inner and outer

closed cyclic contours were taken as cavity-limiting upper and lower boundaries.
[51] H. Nomura, S. Koda, K. Matsumoto, Y. Miyahara, *Stud. Phys. Theor. Chem.* **1983**, *27*, 151–163.
[52] W. Saenger, M. Noltemeyer, *Chem. Ber.* **1976**, *109*, 503–517.
[53] W. Blokzijl, J. B. F. N. Engberts, *Angew. Chem.* **1993**, *105*, 1610–1648; *Angew. Chem. Int. Ed. Engl.* **1993**, *32*, 1545–1579.
[54] D. W. Griffiths, M. L. Bender, *Adv. Catal.* **1973**, *23*, 209–261.
[55] W. Heiden, G. Moeckel, J. Brickmann, *J. Comput.-Aided Mol. Des.* **1993**, *7*, 503–514.
[56] M. Teschner, C. Henn, H. Vollhardt, S. Reiling, J. Brickmann, *J. Mol. Graphics* **1994**, *12*, 98–105.
[57] [57a] J. Brickmann, in: *Software Development in Chemistry* (Ed.: C. Jochum), GDCh Publ., Frankfurt, **1994**, pp. 139–156. – [57b] P. V. Pixner, W. Heiden, H. Merx, G. Moeckel, A. Möller, J. Brickmann, *J. Chem. Inf. Comput. Sci.* **1994**, *34*, 1309–1319.
[58] D. J. Heisterberg, *QTRFIT – Rigid Body Rotation and Fitting Program*, The Ohio Supercomputer Center, Columbus, Ohio 43212, **1991**.
[59] L. Verlet, *Phys. Rev.* **1967**, *159*, 98–103.
[60] [60a] B. R. Brooks, R. E. Bruccoleri, B. D. Olafson, D. J. States, S. Swaminathan, M. Karplus, *J. Comput. Chem.* **1983**, *4*, 187–217. – [60b] L. Nilsson, M. Karplus, *J. Comput. Chem.* **1986**, *7*, 591–616.
[61] [61a] S. M. Kast, K. Nicklas, H.-J. Bär, J. Brickmann, *J. Chem. Phys.* **1994**, *100*, 566–576. – [61b] S. M. Kast, J. Brickmann, *J. Chem. Phys.* **1995**, in press.

[242/94]